

Frozen fronts in cellular flows

M. E. Schwartz* and T. H. Solomon†

*Department of Physics and Astronomy,
Bucknell University, Lewisburg, PA 17837*

(Dated: November 20, 2018)

Abstract

We present experiments on the behavior of reaction fronts in ordered and disordered cellular flows with imposed winds. Fronts in a chain of alternating vortices are found to freeze (pin to the separatrix) for a wide range of imposed winds that grows nonlinearly with the characteristic strength of the underlying vorticity. Experiments in spatially-disordered flows demonstrate that freezing of fronts is common to cellular flows; furthermore, it is not dependent on boundary conditions. We therefore anticipate similar pinning in a wide range of cellular flows and front-producing systems.

PACS numbers: 82.40.Ck, 47.70.Fw, 47.32.C-, 47.54.-r

Numerous chemical, biological and physical systems are characterized by two co-existing phases and by the movement of a front that separates these phases. Front propagation can be used to describe a wide variety of dynamical processes, including natural and industrial chemical processes[1], plasma systems[2], solidification[3], the spreading of a disease in a population[4], and marine ecology systems[5]. The dynamics of front propagation are well-understood in stagnant fluids[6, 7]; an issue of significant current interest[8] is how fluid flows affect the motion of fronts. If a uniform “wind” opposing the front is applied to an otherwise motionless fluid, the front simply propagates at its reaction-diffusion (no flow) velocity minus the wind speed. If the same wind is applied to a fluid with an underlying cellular flow, however, the behavior is dramatically different.

In this Letter, we present experiments showing that cellular flows can freeze the motion of a reaction front against an imposed wind. We study this phenomenon as a function of the strength of the vortex flow. Fronts produced by the ruthenium-catalyzed excitable Belousov-Zhabotinsky (BZ) reaction[9, 10, 11, 12] are studied in both ordered and disordered vortex flows. The flows studied are all time-independent; nevertheless, the experimental results have implications for time-dependent flows as well, since a moving vortex in a time-dependent flow can be viewed in a co-moving reference frame as a stationary vortex with a time-dependent imposed wind. We therefore expect front-freezing to be relevant for a wide range of cellular flows.

In the absence of fluid flows, a front propagates with a reaction-diffusion (RD) velocity given by the well-known FKPP result[6, 7] $v_0 = 2\sqrt{D/\tau}$, where D is the molecular diffusivity and τ is the reaction timescale. In the past 10 years, there has been growing interest in the effects of fluid advection on front propagation. Theoretical[13] and experimental[14] studies have shown that a front propagating against a simple pipe flow moves with velocity v_0 independent of the imposed flow due to no-slip boundary conditions at the walls. No-slip conditions also play a key role in explaining anomalous front velocities in flows through a porous medium[15]. Other theoretical studies of front propagation in advection-reaction-diffusion (ARD) systems include predictions of fractal fronts in open flows with chaotic mixing[16, 17]. Recent theories[18, 19, 20] have extended the standard FKPP theory to general ARD systems; however, these approaches do not account explicitly for the effects of cellular flows. The importance of cellular flow structures, for example, is in evidence in time-periodic vortex chains, which cause fronts to mode-lock to the external forcing[21, 22].

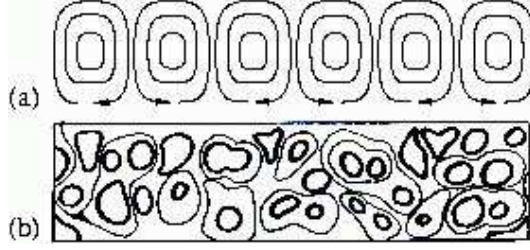


FIG. 1: Schematics of the fluid flow for $\epsilon = 0$ (no flow). (a) Ordered chain of counterrotating vortices. The maximum vortex velocity U is measured at the separatrix. (b) Two-dimensional disordered array.

A mode-locked front propagates an integer number of vortex pairs in an integer number of oscillatory drive periods, inconsistent with straightforward FKPP approaches. Our experiments indicate the fundamental importance of coherent vortices in any general description of ARD dynamics.

Two flows are used for most of these experiments (Fig. 1): a chain of 20 counter-rotating vortices and a random vortex flow, both created using magnetohydrodynamic forcing[23] and confined to an annulus bounded by Plexiglass rings of radii 6.1 and 8.3 cm. A radial current passing through a 2 mm-thick electrolytic solution interacts with a magnetic field produced by Nd-Fe-B magnets below the fluid. Two concentric rings of 3/4"-diameter magnets with alternating polarity are used for the ordered vortex chain and a disordered pattern of 1/4" magnets is used for the random flow. The magnets are mounted on a motor that rotates at a constant rate, thus moving the vortices. In a reference frame moving with the magnets, the vortices are stationary and there is a constant, uniform wind with a velocity W equal to the drift velocity of the magnets.

The electrolytic solution is composed of the chemicals for the excitable Ru-catalyzed BZ reaction[12]. In this reaction, orange Ru^{2+} ions are oxidized to a green Ru^{3+} state, forming a propagating pulse-like front which is imaged using a 12-bit CCD camera with a red interference filter. The Ru-catalyzed BZ reaction is also inhibited by blue-green light. To confine the reaction to the area of interest, we use a video projector to shine blue light everywhere except in the annulus[23]. We also illuminate a small section of the annulus (1-2 vortices) with blue light to control the direction of front propagation. The reaction is triggered with a silver wire on one side of this blinding region; the front cannot propagate

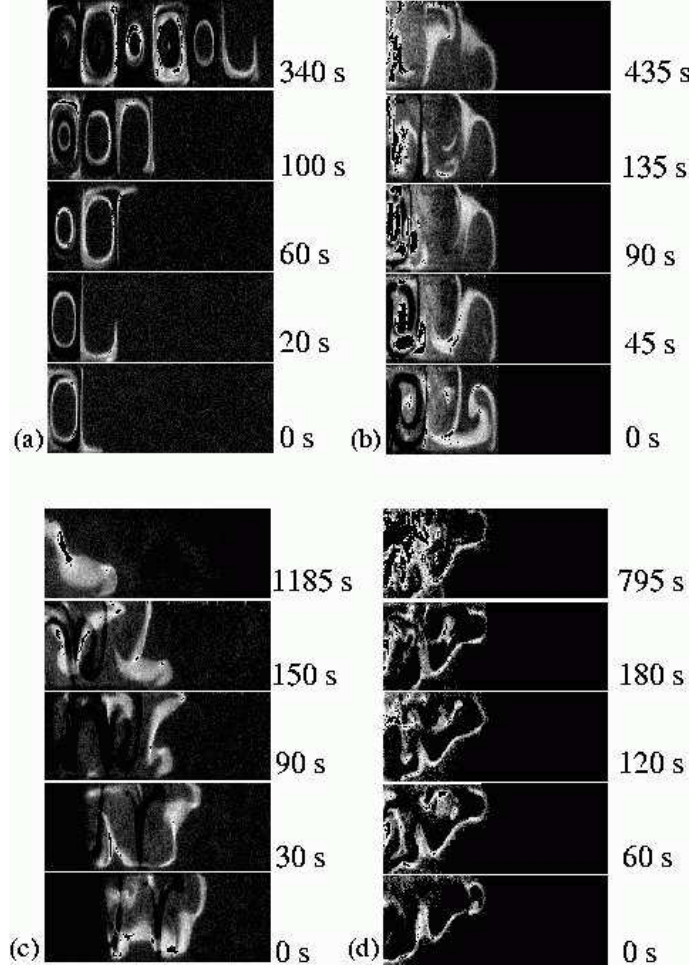


FIG. 2: Sequences of de-curved images, showing regimes of front propagation. In all cases, the imposed wind blows from right to left. (a) Forward-propagating front; $\epsilon = 0$ and $\mu = 40$. The front is advected around the vortex and burns across the separatrix in order to propagate forward. (b) Frozen front; $\epsilon = 2.6$ and $\mu = 12$. The wind prevents the reaction from burning across the separatrix. (c) Backward-propagating front; $\epsilon = 8.6$ and $\mu = 12$. The front is initially in the leading vortex but is blown backwards by the wind. (d) Frozen front for a narrow random array of vortices; $\epsilon = 4.0$ and $\mu = 12$.

through the blinding region and therefore only propagates in one direction. The enhanced images are digitally “de-curved” into a linear chain and shifted into a reference frame moving with the vortices for analysis.

The front velocity v_f , wind speed W , and maximum vortex velocity U are all scaled by the RD velocity: $\nu = v_f/v_0$, $\epsilon = W/v_0$ and $\mu = U/v_0$. In the limit $\mu \rightarrow 0$, the addition of

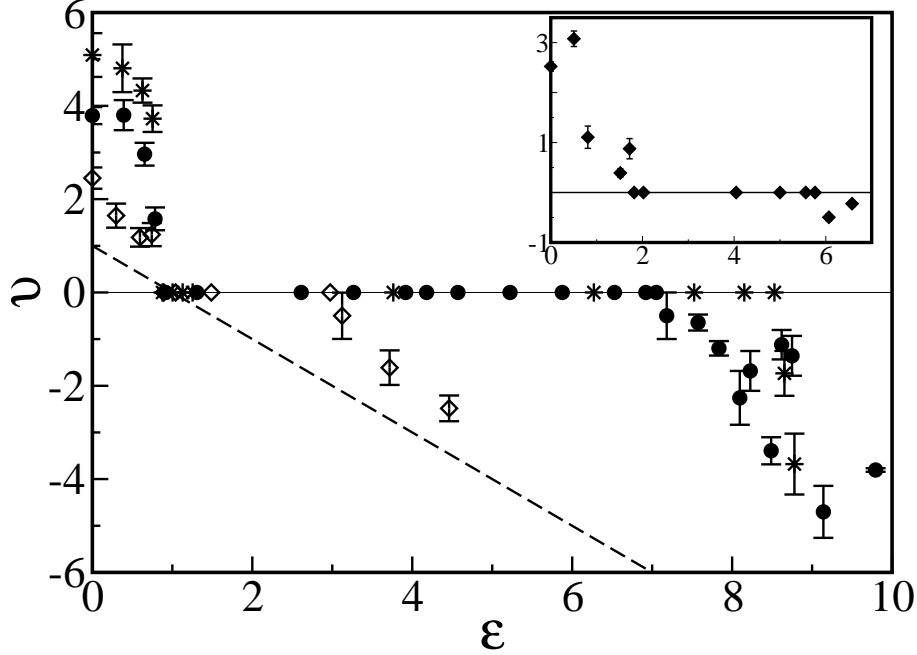


FIG. 3: Front velocities in the face of opposing wind. The data shown is for $\mu = 4, 12$ and 40 (open diamonds, filled circles and stars respectively) along with the theoretical limit (Eq. 1) for $\mu = 0$ (dashed line). The inset shows the same data for a narrow random chain of vortices at $\mu = 12$.

a uniform wind is the equivalent of a Galilean transformation; in a reference frame moving with the wind, there is no flow. Consequently, for $\mu = 0$

$$\nu = 1 - \epsilon \quad (1)$$

In this limit, a front is “frozen” (i.e., $\nu = 0$) only if W is precisely equal to v_0 , i.e. if $\epsilon = 1$.

The addition of underlying vortex structures ($\mu \neq 0$) has a significant effect on front behavior. Sequences of images (Fig. 2) show the regimes of front propagation in this case. In an ordered vortex flow with small ϵ (Fig. 2a), the front propagates forward against the wind; it is advected around each vortex and then burns across the separatrix from one vortex to the next. The front freezes for intermediate wind speeds (Fig. 2b): the wind prevents the front from burning across the separatrix into the next vortex. However, the wind does not blow the front backwards even though ϵ significantly exceeds 1; instead, the front circles in the leading vortex. In the co-moving reference frame of Fig. 2, the front is *frozen*; in any other reference frame, the front is *pinned* to the motion of the leading vortex. For large enough ϵ (Fig. 2c), the front is pushed back by the wind.

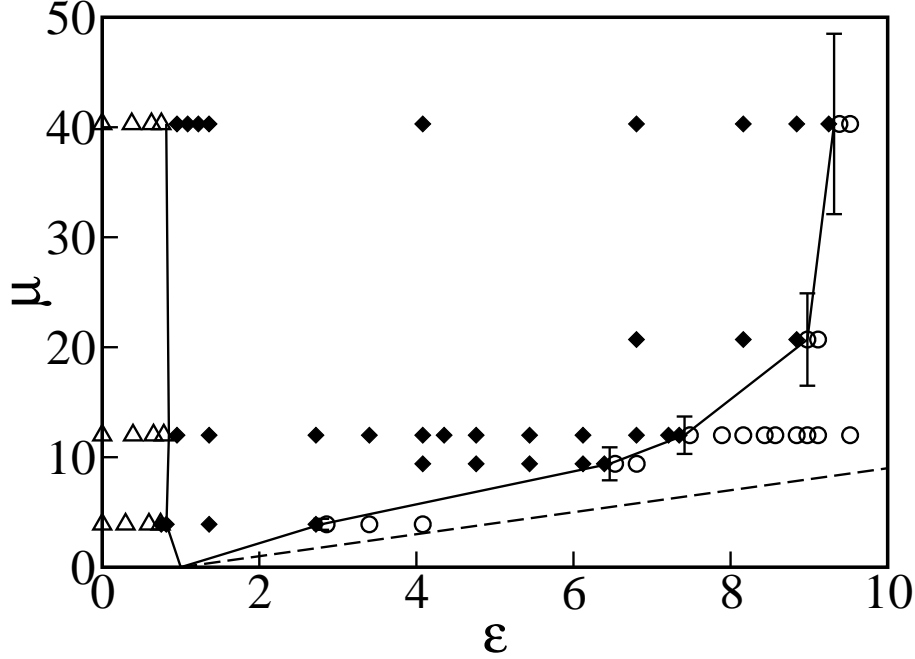


FIG. 4: Parameter-space diagram, showing the increase in the range of the frozen front regime with increasing μ . Open triangles denote forward propagation of the front against the wind, closed diamonds represent pinned fronts, and open circles denote backward (downwind) front propagation. The solid line shows the boundary between pinned and unpinned fronts. The error bars show the uncertainty in μ , which is caused chiefly by uncertainty in U as it increases. The dashed line is at $\epsilon = \mu + 1$, the normalized sum of the RD and advective velocities.

Front velocities in the co-moving reference frame are plotted as a function of the wind speed in Fig. 3 for three values of μ , along with the prediction from Eq. 1 for the $\mu = 0$ limit. The most salient feature of Fig. 3 is the plateau, clearly visible for all three values of μ , where the front velocity $\nu = 0$. The width of the frozen-front plateau decreases with decreasing μ and the velocities approach the theoretical limit as μ approaches 0. Also note that advection due to the vortices enhances the front speeds when $\epsilon < 1$, consistent with previous studies of the $\epsilon = 0$ limit[23, 24, 25].

The variation with μ of the width of the pinned-front regime can be seen in a parameter-space diagram (Fig. 4). The minimum wind speed to achieve frozen fronts is (within error) the RD front velocity: $\epsilon = 1$. This can be understood by considering the behavior near the separatrices, where the wind is perpendicular to the underlying vortex flow and where

forward propagation is not aided by advection. If ϵ exceeds 1, the wind is stronger than the forward-burning RD velocity, and the front stalls at the separatrix. The endpoint of the plateau is significantly below $\mu + 1$ (i.e. the sum of the RD velocity and the advective velocity), and it diverges from this line in a nonlinear fashion. We are currently investigating this nonlinear behavior, particularly in light of secondary flows[26] and no-slip boundary conditions in the experiments.

Frozen fronts are also observed for random vortex flows, as shown in Fig. 2d and the inset of Fig. 3. The freezing mechanism remains the same – the front is pinned at the (more convoluted) separatrices. Several features, however, are different for the random flow. First, the front velocity does not decrease smoothly as ϵ approaches 1, due to the random nature of the flow – different sections of the flow have different characteristic advective speeds. Second, the minimum ϵ necessary for frozen fronts is significantly greater than 1. The separatrices are not typically perpendicular to the wind for random flows; as a result, higher W is required for the perpendicular component of the wind to exceed v_o and thus prevent the front from burning across a separatrix.

Freezing of fronts is not restricted to flows with a limited number of vortices, nor is it dependent on no-slip boundary conditions in a confined geometry. A frozen front is shown in Fig. 5 for a significantly wider annulus (inner and outer radii 2.6 and 8.3 cm), along with a streak photograph showing the underlying disordered pattern of vortices. Due to the annular geometry, W grows by a factor of 3 between the inner and outer edges; despite this increase in W fronts freeze across the entire annulus, a further indication of the robustness of this phenomenon. As seen in Fig. 5b, the frozen front generally follows the separatrices, although it is pushed back slightly from the edge of the vortices at larger radii due to the increased wind.

Our experiments indicate that pinning of reaction fronts should occur in a wide range of steady vortex flows, regardless of the spatial pattern of the vortices. Furthermore, these results help interpret and predict front behavior in time *dependent* flows. We can use front pinning, for example, to explain mode-locking in an oscillating vortex flow[21, 22]. In a co-moving (i.e. oscillating) reference frame, the vortices are stationary in the presence of an oscillating wind. For sufficiently large oscillatory velocity, the wind pins the front to a vortex during a significant fraction of each oscillation period. Thus, the front can only propagate during a well-defined segment of each period, tying the front propagation speed

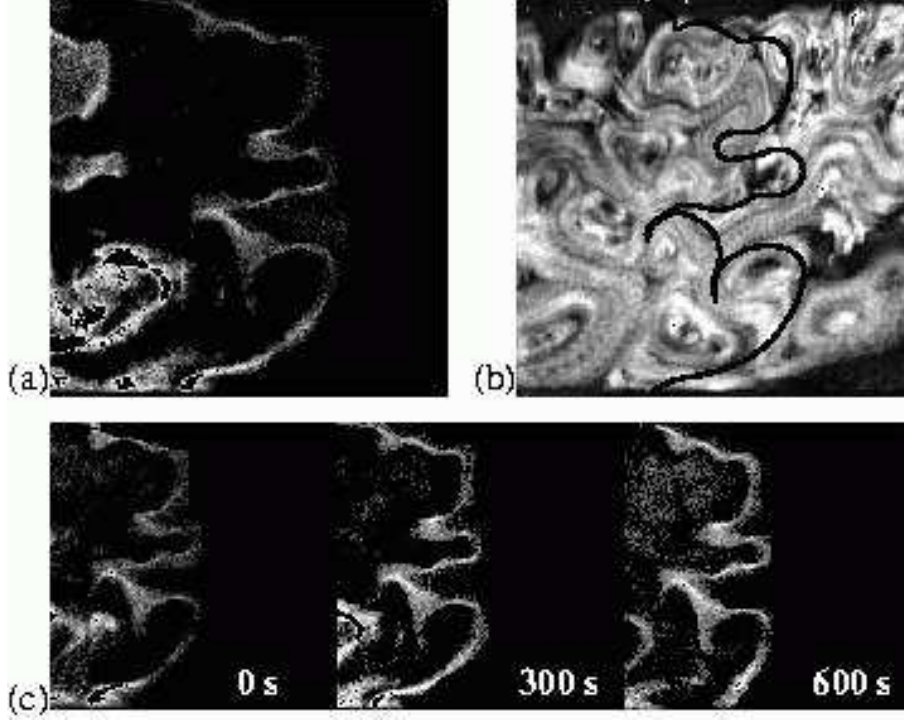


FIG. 5: Frozen front in a wide two-dimensional random array of vortices. The images are de-curled with the inner and outer radii at the bottom and top of the image, respectively. (a) Image of the frozen reaction front. The normalized wind ϵ ranges from 1.8 to 5.8 from the bottom to the top of each image. (b) Streak photograph of the underlying vortex flow with $\epsilon = 0$. The front from (a) (black curve) is superimposed on the section of the flow where it freezes. (c) Snapshots of frozen front.

to the oscillation frequency.

Moving vortices in other time-dependent flows can be expected to pin reaction fronts similarly, if only temporarily, in a manner that fundamentally alters the speed and method of front propagation. Consider the case of a vortex and a front moving in the same direction. If the vortex passes through the front with a sufficient speed, it will pin and drag the front forward. (In the reference frame of the vortex, this is equivalent to the frozen-front case.) Even if the vortex later slows down or speeds up such that it can no longer hold the front, it will have already significantly altered the shape and location of the front. These ideas should extend even to turbulent flows, which are often characterized by both transient and long-lived coherent vortices[27, 28]. Ultimately, any general theory of front propagation in

ARD systems will have to account for pinning of fronts by vortices in the flow.

This work was supported by the US National Science Foundation (grants DMR-0404961, DMR-0703635 and REU-0552790).

* Current address: Department of Physics, Columbia University, New York, NY 10027, USA;
email: mes2140@columbia.edu

† email address: tsolomon@bucknell.edu

- [1] P. Grindrod, *The theory and applications of reaction-diffusion equations: Patterns and Waves* (Clarendon Press, Oxford, 1996).
- [2] D. Beule, A. Forster, and T. Fricke, Int. J. Research Phys. Chem. and Chem. Phys. **204**, 1 (1998).
- [3] D. T. J. Hurle, ed., *Handbook of Crystal Growth*, vol. 1B (North-Holland, Amsterdam, 1993).
- [4] M. N. Kuperman and H. S. Wio, Physica A **272**, 206 (1999).
- [5] E. R. Abraham, C. S. Law, P. W. Boyd, S. J. Lavender, M. T. Maldonado, and A. R. Bowie, Nature **407**, 727 (2000).
- [6] R. A. Fisher, Ann. Eugenics **7**, 355 (1937).
- [7] A. N. Kolmogorov, I. G. Petrovskii, and N. S. Piskunov, Moscow Univ. Bull. Math. **1**, 1 (1937).
- [8] T. Tel, A. de Moura, C. Grebogi, and G. Karolyi, Phys. Rep. **413**, 91 (2005).
- [9] A. T. Winfree, Science **175**, 634 (1972).
- [10] K. Showalter, J. Chem. Phys. **73**, 3735 (1980).
- [11] R. J. Field and M. Burger, *Oscillations and Traveling Waves in Chemical Systems* (Wiley, New York, 1985).
- [12] M. Tinsley, J. X. Cui, F. V. Chirila, A. Taylor, S. Zhong, and K. Showalter, Phys. Rev. Lett. **95**, 038306 (2005).
- [13] B. F. Edwards, Phys. Rev. Lett. **89**, 104501 (2002).
- [14] M. Leconte, J. Martin, N. Rakotomalala, and D. Salin, Phys. Rev. Lett. **90**, 128302 (2003).
- [15] M. Kaern and M. Menzinger, J. Phys. Chem. B **106**, 3751 (2002).
- [16] Z. Neufeld, Phys. Rev. Lett. **87**, 108301 (2001).
- [17] Z. Toroczkai, G. Karolyi, A. Pentek, T. Tel, and C. Grebogi, Phys. Rev. Lett. **80**, 500 (1998).

- [18] R. Mancinelli, D. Vergni, and A. Vulpiani, *Europhys. Lett.* **60**, 532 (2002).
- [19] D. del Castillo-Negrete, B. A. Carreras, and V. E. Lynch, *Phys. Rev. Lett.* **91**, 018302 (2003).
- [20] D. Brockmann and L. Hufnagel, *Phys. Rev. Lett.* **98**, 178301 (2007).
- [21] M. Cencini, A. Torcini, D. Vergni, and A. Vulpiani, *Phys. Fluids* **15**, 679 (2003).
- [22] M. S. Paoletti and T. H. Solomon, *Euro. Phys. Lett.* **69**, 819 (2005).
- [23] M. S. Paoletti and T. H. Solomon, *Phys. Rev. E* **72**, 046204 (2005).
- [24] M. Abel, A. Celani, D. Vergni, and A. Vulpiani, *Phys. Rev. E* **64**, 046307 (2001).
- [25] A. Pocheau and F. Harambat, *Phys. Rev. E* **64**, 046307 (2006).
- [26] T. H. Solomon and I. Mezić, *Nature* **425**, 376 (2003).
- [27] J. Sommeria, S. D. Meyers, and H. L. Swinney, *Nature* **331**, 689 (1988).
- [28] P. S. Marcus, *Nature* **331**, 693 (1988).